JCB Article

Regulation of presynaptic phosphatidylinositol 4,5-biphosphate by neuronal activity

Kristina D. Micheva,[1] Ronald W. Holz,[2] and Stephen J. Smith[1]

[1]Department of Molecular and Cellular Physiology, Stanford University, Stanford, CA 94305
[2]Department of Pharmacology, University of Michigan Medical School, Ann Arbor, MI 48109

Phosphatidylinositol 4,5-biphosphate (PIP2) has been implicated in a variety of cellular processes, including synaptic vesicle recycling. However, little is known about the spatial distribution of this phospholipid in neurons and its dynamics. In this study, we have focused on these questions by transiently expressing the phospholipase C (PLC)-δ1 pleckstrin homology (PH) domain fused to green fluorescent protein (GFP) in cultured hippocampal neurons. This PH domain binds specifically and with high affinity to PIP2. Live confocal imaging revealed that in resting cells, PH-GFP is localized predominantly on the plasma membrane. Interestingly, no association of PH-GFP with synaptic vesicles in quiescent neurons was observed, indicating the absence of detectable PIP2 on mature synaptic vesicles. Electrical stimulation of hippocampal neurons resulted in a decrease of the PH-GFP signal at the plasma membrane, most probably due to a PLC-mediated hydrolysis of PIP2. This was accompanied in the majority of presynaptic terminals by a marked increase in the cytoplasmic PH-GFP signal, localized most probably on freshly endocytosed membranes. Further investigation revealed that the increase in PH-GFP signal was dependent on the activation of N-methyl-D-aspartate receptors and the consequent production of nitric oxide (NO). Thus, PIP2 in the presynaptic terminal appears to be regulated by postsynaptic activity via a retrograde action of NO.

Introduction

The phospholipid phosphatidylinositol 4,5-biphosphate (PIP2)* has been implicated in a variety of cellular processes, including the production of intracellular messengers, cytoskeletal regulation, and vesicular traffic (Martin, 1998; Toker, 1998; Corvera et al., 1999; Cremona and De Camilli, 2001). PIP2 plays an important role in these processes, either as a substrate for enzymes such as lipid kinases and phosphatases, or through direct interactions with several proteins.

In the process of synaptic vesicle recycling, PIP2 has been found to interact with numerous proteins involved in exo- or endocytosis. PIP2 binds to synaptotagmin in the presence of a Ca^{2+} concentration typically found in the presynaptic terminal of a stimulated neuron, and this reaction could be involved in the docking of synaptic vesicles (Schiavo et al., 1996). PIP2 also binds to rabphilin 3 (Chung et al., 1998), a possible effector of the small GTPases Rab3A and Rab3C, which have been postulated to control the formation of the SNARE complex. Other relevant interactions include the binding of PIP2 to the Mint proteins, which have been implicated in docking (Okamoto and Sudhof, 1997), and to the calcium-dependent activator protein for secretion involved in the secretion of dense core vesicles (Loyet et al., 1998), as well as the inhibition by PIP2 of the synaptic vesicle protein casein kinase I, which phosphorylates a subset of vesicle proteins, including synaptic vesicle protein 2 (Gross et al., 1995). At least some, if not all of these interactions are physiologically relevant, since PIP2 is required for the ATP-dependent priming step preceding exocytosis (Holz et al., 1989; Eberhard et al., 1990; Hay et al., 1995; Wiedemann et al., 1998). PIP2 involvement in the endocytic loop seems equally complicated. Studies in permeabilized cells reveal that PIP2 is required both in the early and late stages of clathrin-mediated endocytosis (Jost et al., 1998). Indeed, PIP2 has been found to interact with many endocytic proteins, such as AP2, epsin, and AP180, this being essential for the formation of clathrin-coated pits (Gaidarov and Keen, 1999; Ford et al., 2001; Itoh et al., 2001). PIP2 also binds

Address correspondence to Kristina D. Micheva, Department of Molecular and Cellular Physiology, Stanford University, 279 Campus Dr., Stanford, CA 94305. Tel.: (650) 725-7552. Fax: (650) 725-8021. E-mail: kmicheva@stanford.edu

*Abbreviations used in this paper: carboxy-PTIO, 2-(4-carboxyphenyl)-4,4,5,5-tetramethylimidazoline-1-oxyl-3-oxide, potassium salt; DEANO, diethylamine NO; div, days in vitro; DTT, dithiothreitol; GFP, green fluorescent protein; IP3, inositol 1,4,5-trisphosphate; NGS, normal goat serum; NMDA, N-methyl-D-aspartate; NMDAR1, NMDA receptor 1; NO, nitric oxide; NOS, NO synthase; PAO, phenylarsine oxide; PH, pleckstrin homology; PHM, PH mutant; PIP2, phosphatidylinositol 4,5-biphosphate; TRIM, 1-(2-trifluoromethylphenyl) imidazole.

Key words: phosphatidylinositol 4,5-biphosphate; green fluorescent protein; synapse; NMDA; nitric oxide

to dynamin (Lin and Gilman, 1996; Zheng et al., 1996), which is recruited to the neck of the invaginating clathrin-coated vesicle, possibly to effect vesicle closure by activating its downstream effector, endophilin I (Schmidt et al., 1999). Synaptojanin, another protein involved in endocytosis, is a PI 5-phosphatase that converts PIP2 into PIP (McPherson et al., 1996), and this reaction appears to be important for uncoating of the endocytic vesicles (Cremona et al., 1999).

An important prerequisite for better understanding the role of PIP2 in synaptic vesicle recycling is knowledge of the spatial distribution of this phospholipid and its dynamics. In this respect, there are limited data available in the current literature. Although it is well known that PIP2 is enriched in the plasma membrane (Hokin and Hokin, 1964; Eichberg and Dawson, 1965), it is not yet clear whether it is present at the synaptic vesicle membrane as well. Also, very little is known about the changes in PIP2 concentration during synaptic activation (Waring et al., 1999). In the present study, we have focused on these questions by transiently expressing the PLC-δ PH domain fused to green fluorescent protein (GFP) in cultured hippocampal neurons. This PH domain binds specifically and with high affinity to PIP2 (Paterson et al., 1995) and its fusion with GFP has been used to study the in vivo distribution of PIP2 in several nonneuronal types of cells (Stauffer et al., 1998; Varnai and Balla, 1998; Botelho et al., 2000; Holz et al., 2000; Raucher et al., 2000).

Results

PH-GFP is concentrated at the neuronal plasma membrane, but not at mature synaptic vesicles

PH-GFP, when transiently transfected into neurons, labeled the plasma membrane of cell bodies and neuronal processes (Fig. 1 A). A weaker, diffuse cytoplasmic staining was also detected. The pattern of PH-GFP staining was identical to the pattern of PIP2 distribution in the nontransfected cell, as detected by a monoclonal PIP2 antibody in fixed cells (Fig. 1 B). As an additional control for the specificity of the PH-GFP labeling, neurons were transfected with a GFP fusion to a PH domain with a point mutation in the region defined as the binding site to PIP2. No plasma membrane distribution was observed in this case (Fig. 1 C), indicating that the characteristic PH-GFP localization reflects the binding of the PH domain to PIP2. Accordingly, a series of photobleaching experiments revealed the lower mobility of PH-GFP compared with PH mutant (PHM)-GFP (Fig. 2). Thus, after equal exposures to laser light, a greater portion of PH-GFP was photobleached compared with PHM-GFP, indicating that fewer fluorescent PH-GFP molecules were diffusing from nonbleached surroundings. Also, as expected, the recovery of PH-GFP was much slower.

An important question is whether PIP2 is localized to synaptic vesicles. To address this question, we labeled synaptic vesicles of transfected neurons with the fluorescent dye FM 4-64. Images for analysis were taken ~20 min or more after the loading procedure to ensure that the synapses were in quiescent state. In large presynaptic varicosities (2–3-μm cross-section) in which we could resolve cytoplasm and plasma membrane, PH-GFP was concentrated on the plasma membrane, similarly to the immunolabeled axonal

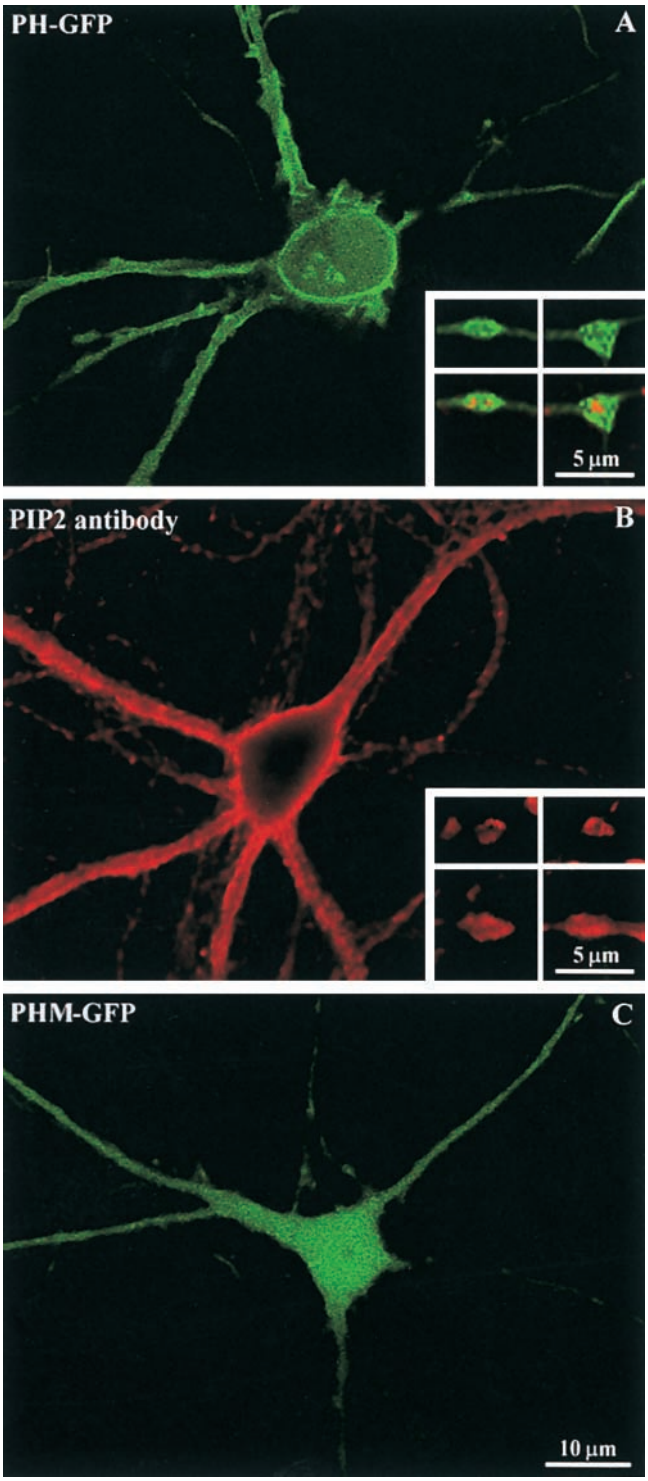

Figure 1. **PH-GFP as a marker for PIP2 in live neurons.** Live hippocampal neurons (8 div) in culture transfected with PH-GFP (A) or PHM-GFP (C). Note the membrane distribution of the PH-GFP signal, which is identical to the distribution of PIP2 as detected by a monoclonal antibody in fixed neurons (B). The inset in A shows the PH-GFP distribution in two large presynaptic varicosities (top) loaded with the dye FM 4-64 (red signal superimposed on the GFP signal in the lower panels). The images were taken ~20 min after the electrical stimulation used for FM loading, i.e., they correspond to synapses in quiescent state. The red and green signals appear to be mutually exclusive, suggesting the absence of PIP2 on synaptic vesicles in quiescent synapses. The inset in B shows the membrane distribution of PIP2 in axonal varicosities, as detected by immunochemistry.

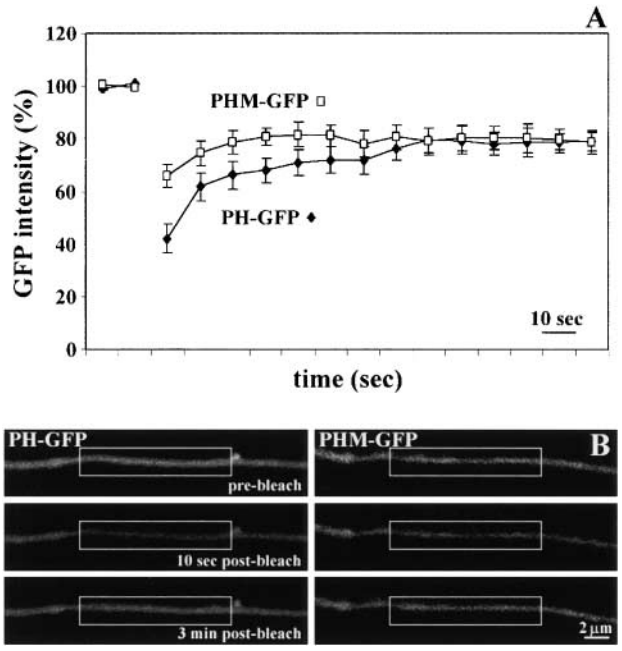

Figure 2. **Photobleach-recovery analysis of the mobility of PH-GFP and PHM-GFP.** (A) Normalized fluorescence recovery curves of PH-GFP and PHM-GFP. Error bars show standard errors. (B) Axons of neurons transfected with PH-GFP (left) and PHM-GFP (right) imaged before and after photobleaching. The box indicates the photobleached area. Note the higher degree of bleaching in the case of PH-GFP.

varicosities (Fig. 1, A and B, insets). More interestingly, FM 4-64 and PH-GFP staining appeared mutually exclusive, suggesting a lack of significant amounts of PIP2 on synaptic vesicles of quiescent synapses (Fig. 1 A, inset). The grainy appearance of the GFP fluorescence on Fig. 1, A and C, as well as on the following figures is due to photon noise, since imaging at a much higher zoom and power did not reveal similar heterogeneities in the GFP distribution (data not shown). To protect the neurons, lower power and zoom where used for imaging in the course of live experiments.

PH-GFP transfection does not affect the viability of neurons, their overall morphology, or the ability for exo- and endocytosis of synaptic vesicles

Using PH-GFP as a marker for the distribution of PIP2 in live neurons requires that this construct not interfere with basic cellular functions. In this respect, several parameters were monitored: cell viability, morphology, actin polymerization, and synapse formation and function.

Neurons transiently transfected at different ages (between 4 to 15 d in vitro) were used in experiments for up to 8 d after transfection. No preferential cell death was observed in the transfected population compared with the rest of the neurons. The morphology of transfected neurons also did not appear to differ from that of the remaining neurons when comparing their dendrite branching pattern and axon extension (Fig. 3).

Since PIP2 is thought to be an important regulator of the actin cytoskeleton, we also compared the degree of actin polymerization in transfected and nontransfected neurons. Staining with Alexa phalloidin revealed that, as expected, the degree of actin polymerization was on the average 22% lower in transfected neurons (1,970 ± 133 arbitrary units of phalloidin intensity in transfected cells versus 2,520 ± 102 arbitrary units in control cells; $P < 0.01$, two sample t tests). However, this did not appear to affect the morphology of neurons (see above).

Synapse formation and function were assessed by FM 4-64 labeling of live cultures. The number of synapses, as identified by FM 4-64 labeling, varied greatly along axons and between different axons both in transfected and nontransfected neurons. For the analysis of synaptic numbers, we looked only at what appeared to be individual axons running through the field. Three general cases were observed: long stretches of axons not making any synapses, regions of axons making an occasional synapse, and regions of axons forming strings of relatively uniformly spaced synapses. For analysis we chose only those regions of axons that formed strings of synapses (such as on Fig. 4). No statistically significant difference in the number of synapses was observed when comparing transfected and nontransfected axons, regardless of the age. Thus, already at 6 d in vitro (div) there were 0.22 ± 0.02 (mean ± SEM) synapses per 1 μm in control axons compared with 0.20 ± 0.01 synapses per 1 μm in transfected axons. With age, the number of synapses slightly increased to reach a plateau: 0.25 ± 0.01 per 1 μm in control axons and 0.26 ± 0.01 per 1 μm in transfected axons at 8–9 div; and 0.27 ± 0.01 per 1 μm in control axons and 0.26 ± 0.02 per 1 μm in transfected axons at 15–16 div. The FM 4-64 experiments were also used to estimate whether transfection had any effect on the number of recycling vesicles per synapse. The intensity of FM 4-64 loading (initial FM values minus residual FM values obtained after "unloading") is expected to be proportional to the number of vesicles that have taken up the dye, i.e., the vesicles that have undergone exo- and endocytosis upon a particular stimulation. After electrical stimulation (30 s at 10 Hz), the intensity of FM 4-64 loading of synapses varied greatly both in transfected and nontransfected synapses. However, the average intensity of FM 4-64 loading of synapses was essentially the same: 802 ± 30 arbitrary units for control synapses ($n = 255$) and 795 ± 31 arbitrary units for transfected synapses ($n = 173$) in cultures 9–13 div.

Thus, except for somewhat reducing the level of polymerized actin in transfected neurons, PH-GFP does not seem to noticeably interfere with essential cellular functions, such as cell survival, growth, synapse formation, or function, and therefore can be used to monitor the distribution of PIP2 in live cells.

Electrical stimulation causes an increase in the GFP fluorescence in presynaptic boutons

If PIP2 were involved in synaptic vesicle recycling, one might expect to see a change in its pattern of distribution and/or concentration in synapses upon electrical stimulation. Based on this assumption, we conducted the following experiment: neuronal cultures were loaded with FM 4-64 and regions of transfected axons with active synapses were imaged during rest and during electrical stimulation. Subsequent analysis revealed that stimulation caused an increase in the average GFP intensity of the imaged population of transfected presynaptic boutons (Figs. 4 and 5). This effect was

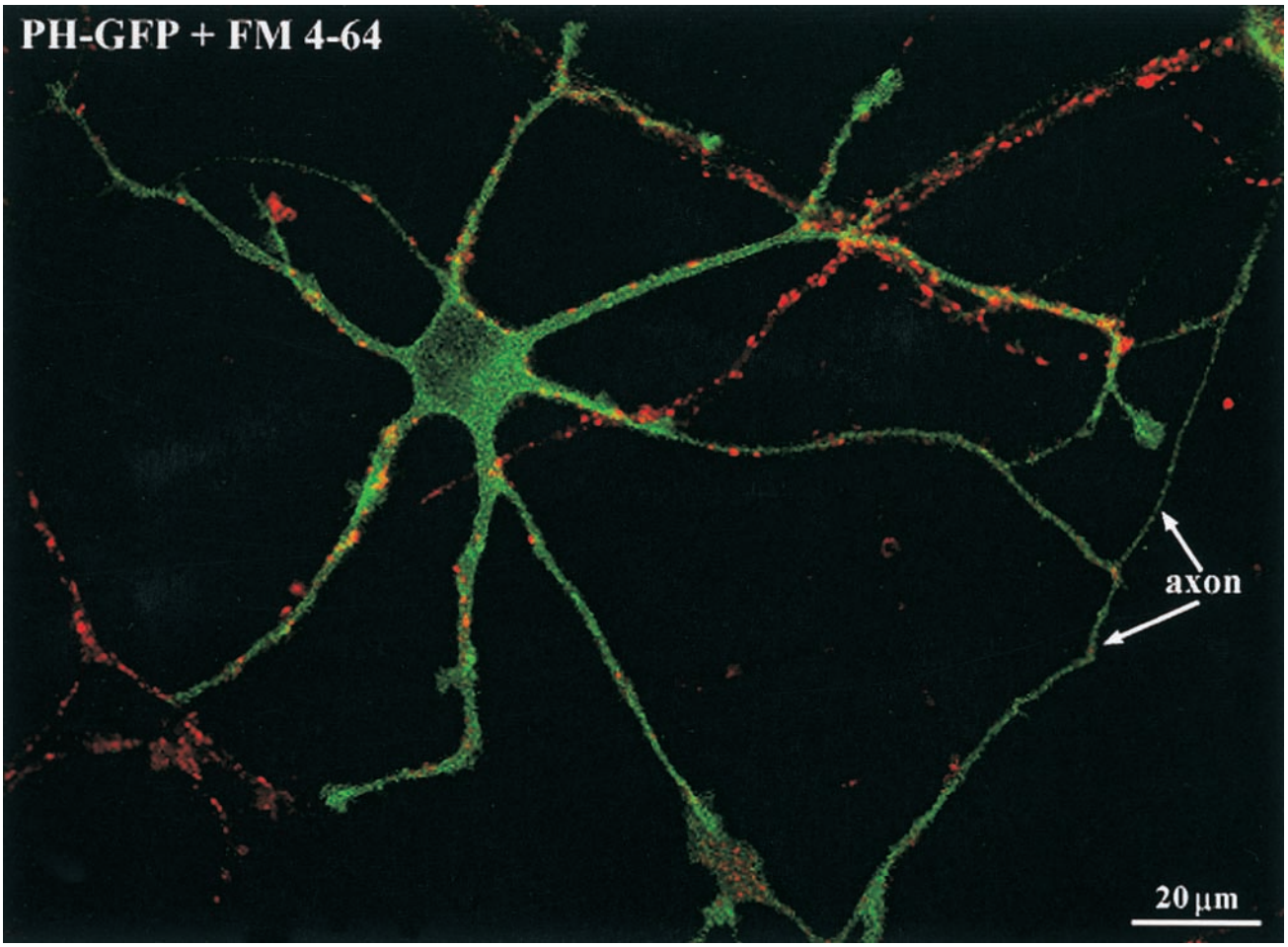

Figure 3. **Synaptic innervation of a live hippocampal neuron transfected with PH-GFP.** The neuron (10 div) displays a normal dendrite branching pattern and has a bifurcating axon extending beyond the field of view. Numerous synapses as identified by FM 4-64 loading (red) are contacting the dendrites and cell body. Synapses on other nontransfected neuronal processes are also seen.

particularly obvious when compared with the changes in GFP intensity in neurons transfected with the mutant construct PHM-GFP. Thus, although the average GFP intensity in presynaptic boutons or neurons transfected with PH-GFP increased by ~10%, it actually decreased on the average by 20% in the control case. The decrease in GFP intensity upon electrical stimulation in the control presynaptic boutons is expected due to the pH sensitivity of GFP (Patterson et al., 1997). To verify the dependence of GFP fluorescence on the acidity of the environment in our system, we fixed, permeabilized, and imaged neurons transfected with PHM-GFP in solutions of different pH. The intensity of GFP remained stable between pH 7.6 and 7.2, and then decreased with acidification of the medium (Fig. 5 C). At about pH 6.7, the intensity of GFP dropped to 80% of that observed at pH 7.4, which corresponds to the decrease in GFP intensity upon electrical stimulation of neurons transfected with PHM-GFP. This is in good accord with previous studies showing that prolonged neuronal activity causes intracellular acidification (Chesler and Kaila, 1992; Zhan et al., 1998; Xiong et al., 2000). In the PH-GFP–transfected neurons, increased GFP fluorescence was observed only in presynaptic boutons, as identified using FM 4-64. In contrast, axonal regions adjacent to the boutons, postsynaptic sites, dendrites, and cell bodies all displayed a decrease in GFP fluorescence, similar to the control PHM-GFP–transfected presynaptic boutons. The response of the PH-GFP–transfected presynaptic boutons to electrical stimulation was heterogeneous, with some boutons increasing their GFP-intensity as much as 100%, while others slightly decreased (Fig. 5 D). Of the analyzed presynaptic boutons, 61% (72 out of 118) showed an increase in GFP fluorescence, and from these 24% (17 out of 72) increased their GFP fluorescence by >50%. The onset and duration of the effect also varied, but on the average it took ~20 s for an increase in GFP fluorescence to be observed and it returned to baseline after ~4 min, i.e., 2 min after the end of a 2 min stimulation of 10 Hz. The increase in GFP fluorescence in presynaptic boutons could be reproduced in consecutive rounds of stimulation (Fig. 5 E).

The number of recycled vesicles is larger at boutons that show an increase in PH-GFP fluorescence

To assess the functional significance of the PH-GFP fluorescence changes in presynaptic boutons during electrical stimulation, we studied the association between the increase in PH-GFP and the amount of FM 4-64 loading of presynaptic boutons. Neuronal cultures transfected with PH-GFP were loaded with FM 4-64 by electrical stimulation of 10 Hz for

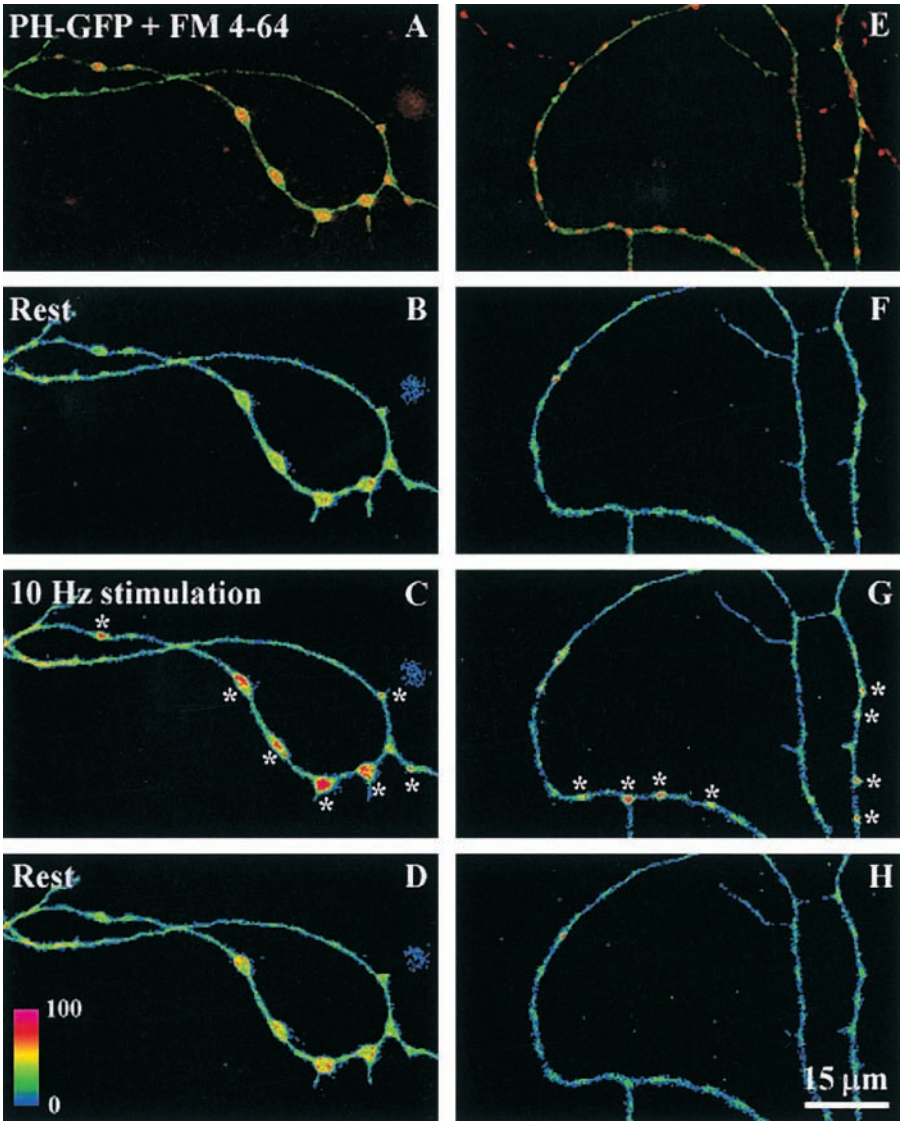

Figure 4. **Increase in the PH-GFP fluorescence of presynaptic boutons upon electrical stimulation.** (A and E) Axons of hippocampal neurons, transfected with PH-GFP (green), and loaded with FM 4-64 (red). (B–D and F–H) Pseudocolor images of the same axons in the GFP channel, showing the changes in GFP fluorescence upon electrical stimulation. Presynaptic boutons, which increased their GFP fluorescence, are labeled with asterisks. Pseudocolor scale in D, numbers represent fluorescence intensity in arbitrary units.

30 s. Regions of transfected axons loaded with FM 4-64 were then selected and imaged during rest and electrical stimulation. The percentage increase in PH-GFP intensity and the FM 4-64 loading were positively correlated with a correlation coefficients varying between 0.11 and 0.48 for the individual experiments ($n = 140$ from five experiments). An example of such an experiment is shown in Fig. 6 A. Even though this correlation was weak, there was a statistically significant difference between the amount of FM 4-64 loading of synapses that showed an increase in PH-GFP fluorescence and the ones that did not (Fig. 6 B). Thus, the presynaptic boutons where PH-GFP fluorescence increased upon stimulation had on average a 30% higher FM 4-64 loading ($P < 0.01$, two sample t test). Since the intensity of FM 4-64 loading is proportional to the number of recycled vesicles, this indicates that the number of recycled vesicles is larger at boutons that show an increase in PH-GFP fluorescence.

Electrical stimulation also causes redistribution in the PH-GFP fluorescence pattern of presynaptic boutons

The size of presynaptic boutons in these cultures is usually too small to permit much spatial resolution of substructure at the light level. However, occasionally we encountered larger presynaptic varicosities, up to 2–3 μm in diameter, where the plasma membrane distribution of PH-GFP was apparent at resting state. To achieve a better understanding of the dynamics of presynaptic PIP2, these varicosities were observed at higher magnification (pixel size of 0.121 μm vs. 0.286 μm for the other experiments, three z-sections spaced 0.5 μm apart taken at each time point). Interestingly, in these presynaptic varicosities the characteristic plasma membrane distribution of PH-GFP disappeared immediately after the onset of electrical stimulation (Fig. 7). There followed an increase in GFP fluorescence in the interior of the varicosities, and often an overall increase in the GFP fluorescence of the varicosities. After the end of stimulation, the initial resting pattern of GFP fluorescence was gradually restored, following usually a similar time course to that described for the changes in GFP fluorescence in the overall synaptic population. The observed changes in the location and intensity of PH-GFP cannot be accounted for only by a decrease in the PIP2 amount on the plasma membrane and accumulation of unbound PH-GFP within the cytoplasm, because the overall intensity of the majority of presynaptic

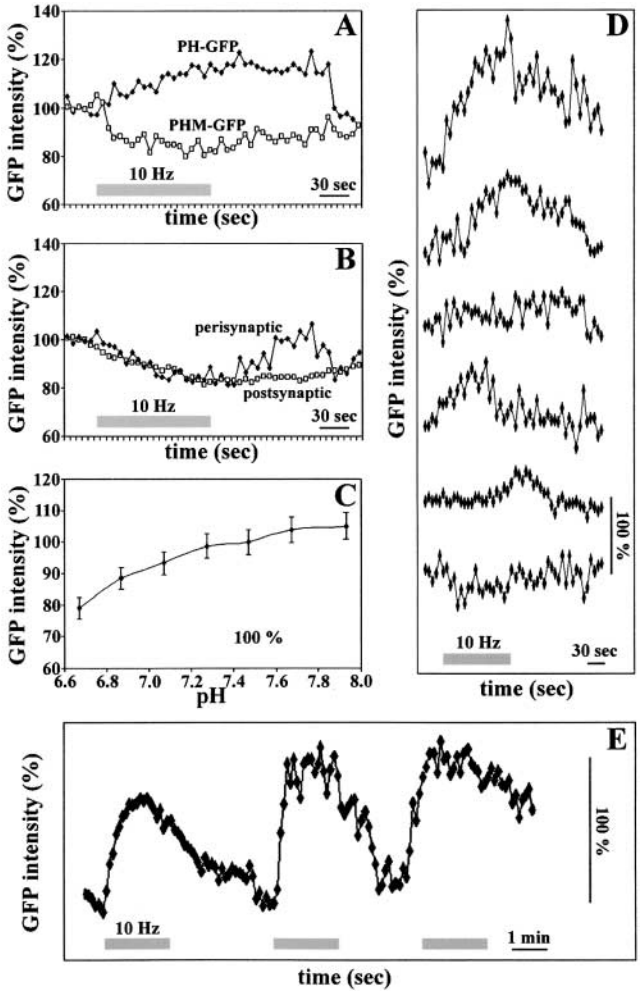

Figure 5. **PH-GFP fluorescence in stimulated neurons.** (A) Changes in GFP fluorescence upon electrical stimulation in presynaptic boutons of neurons transfected with PH-GFP and PHM-GFP. Values of GFP intensity were averaged across the synaptic population and normalized relative to the initial resting state (first five frames). Representative individual experiments are shown for each case, with all synapses within the imaged field being analyzed (n = 39 for PH-GFP, n = 20 for PHM-GFP). (B) Changes in GFP fluorescence of perisynaptic and postsynaptic sites of neurons transfected with PH-GFP upon electrical stimulation. Similar to A, the graph shows representative individual experiments. Only synapses showing an increase in PH-GFP intensity were chosen for the analysis of perisynaptic sites (n = 27). All postsynaptic sites within the field of view were analyzed (n = 16). (C) Dependence of the intensity of GFP fluorescence on the pH of the surrounding medium. Error bars show standard errors. (D and E) Changes in GFP fluorescence of individual presynaptic boutons of neurons transfected with PH-GFP. Values of GFP intensity were normalized relative to the initial resting state (first five frames). Note the great variability in the size and timing of GFP intensity changes.

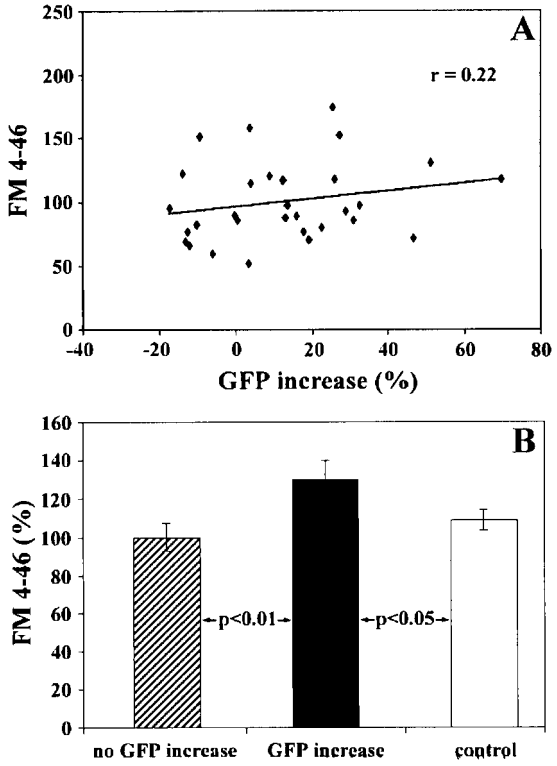

Figure 6. **Relationship between the changes in PH-GFP fluorescence of presynaptic boutons and the number of recycled vesicles.** (A) FM 4-64 loading (arbitrary units) related to the increase in PH-GFP (%) in presynaptic boutons during electrical stimulation. Results from one representative experiment are shown (n = 30; r, correlation coefficient). (B) FM 4-64 labeling of PH-GFP–transfected presynaptic boutons and control boutons. The transfected boutons were divided into two populations: those that increased their PH-GFP intensity upon electrical stimulation (GFP increase), and those that did not (no GFP increase). To be able to pool the data from separate experiments, the FM 4-64 values of all presynaptic boutons of a given experiment were normalized relative to the average FM 4-64 loading of the boutons showing no increase in GFP fluorescence of that particular experiment. The P values for the statistical significance of the differences are shown between the respective bars. n = 87 for each of the two populations of transfected boutons, and n = 255 for the control boutons.

boutons increased (see also Discussion). Rather, taking into account the relatively high mobility of PH-GFP (Fig. 2), the above-described events can be explained by a diffusional recruitment of PH-GFP from adjacent areas due to an increased concentration of PIP2 in the varicosities' interior.

The increase in PH-GFP intensity occurred in the core of presynaptic boutons, similar to the steady state FM 4-64 distribution (for example, compare Figs. 4, A and C, 7, A and D, and 8, C and G). Therefore, this increase in PH-GFP intensity appears to colocalize with the pool of freshly endocytosed vesicles, suggesting that they are enriched in PIP2. After the end of electrical stimulation (Fig. 7 E), the PH-GFP intensity in the interior of presynaptic terminals gradually decreased to reach levels typical of the prestimulation state, when there was an inverse relationship between the PH-GFP and FM 4-64 signals (Fig. 1 A, inset). Thus, our results strongly suggest that electrical stimulation causes a redistribution of PIP2 from the plasma membrane to the interior of presynaptic boutons, most probably on freshly endocytosed vesicles. Maturation of these endocytosed vesicles into synaptic vesicles then leads to a gradual loss of PIP2.

Effect of PLC inhibition on the GFP fluorescence of stimulated presynaptic boutons

The observed increase in GFP fluorescence in presynaptic boutons could potentially be due to an increase in the con-

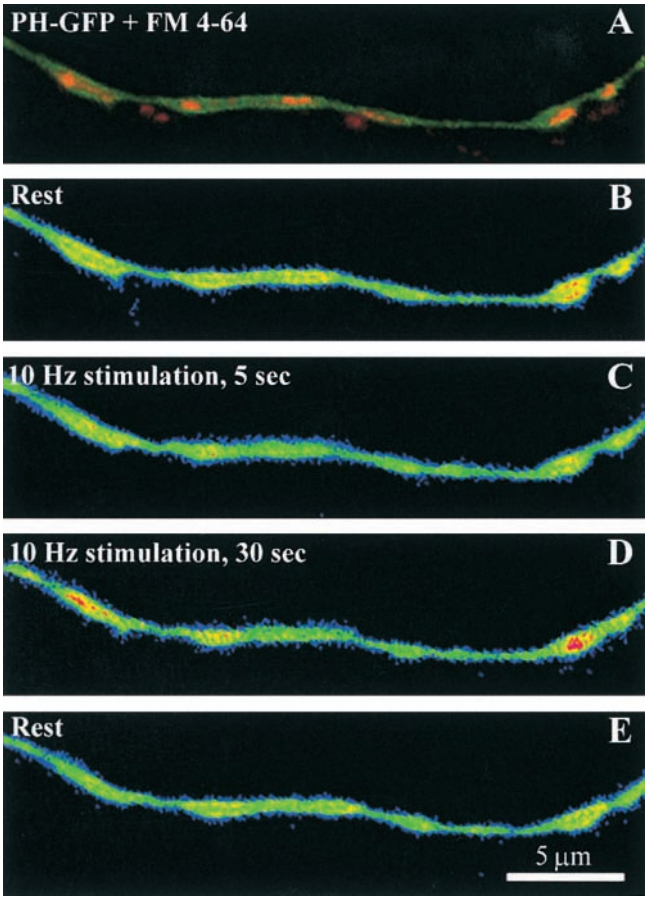

Figure 7. **Changes in the distribution of PH-GFP in presynaptic boutons upon electrical stimulation**. (A) Axon of a hippocampal neuron (10 div), transfected with PH-GFP (green) and loaded with FM 4-64 (red). (B–E) Pseudocolor images of the same axon in the GFP channel, showing the changes in GFP fluorescence upon electrical stimulation. Note the loss of membrane distribution of the GFP signal immediately after the onset of electrical stimulation (C) and the subsequent increase in the GFP fluorescence in some presynaptic varicosities (D). After cessation of the electrical stimulation, the pattern of GFP fluorescence characteristic for the resting state was gradually restored (E).

centration of inositol 1,4,5-trisphosphate (IP3), which also binds with high affinity to the PH domain. If this were the case, inhibiting the PLC-mediated hydrolysis of PIP2 to IP3 and diacylglycerol will eliminate, or at least reduce, the increase in GFP fluorescence in boutons. However, the PLC inhibitor U73122 did not affect the increase in the GFP fluorescence of stimulated boutons (Fig. 8, A, C, E, and G). The GFP fluorescence in presynaptic boutons of transfected neurons was monitored during two consecutive rounds of electrical stimulation, first without and then with U73122 (1 μM; $n = 96$ from five experiments). The same experiment was also performed with the inactive analogue U73343 ($n = 108$ from five experiments). A similar pattern of GFP fluorescence was observed with both reagents. Thus, the increase in GFP fluorescence in stimulated presynaptic boutons is most likely due to an increase in the concentration of PIP2 and not to competitive binding of the PH domain to IP3.

Another possible effect of inhibiting PLC could be a change in the redistribution of PH-GFP in stimulated presynaptic boutons. Thus, if activation of PLC by stimulation were responsible for the hydrolysis of the plasma membrane PIP2 in presynaptic boutons, then inhibition of PLC would prevent or significantly decrease the loss of the plasma membrane localization of PH-GFP. To address this question, we analyzed large presynaptic varicosities at rest and during electrical stimulation, and in the presence or absence of the PLC inhibitor U73122 or the positive control U73343 (Fig. 8 B). Statistical analysis (paired t test) revealed that in all three conditions (untreated, PLC inhibitor, and inactive analogue), the GFP signal decreased on the plasma membrane of presynaptic boutons upon stimulation. However, in the presence of the PLC inhibitor this decrease was significantly smaller compared with the two other conditions (10% vs. 30%, $P < 0.01$, two sample t test). Taking into account the pH dependence of the GFP signal, this small decrease of the GFP fluorescence in the presence of the PLC inhibitor was actually indicative of an increase in PH-GFP content. Electrical stimulation caused an increase in the GFP signal in the cytoplasm in all three conditions, confirming the conclusion from the low magnification experiments that PLC inhibition does not interfere with the increase in GFP fluorescence. This analysis suggests that, under normal conditions, electrical stimulation leads to two parallel processes: activation of PLC in presynaptic boutons, which results in hydrolysis of the plasma membrane PIP2, and increase in the total concentration of PIP2 in the cytoplasm of presynaptic boutons.

Newly synthesized PIP2 is required for the increase in GFP fluorescence in presynaptic boutons upon electrical stimulation

We were further interested in the question of whether the increase in presynaptic GFP fluorescence upon electrical stimulation actually depends on the synthesis of new PIP2 and/or the transport of preexisting PIP2 from adjacent regions. To address this issue, we used phenylarsine oxide (PAO), an inhibitor of the PI-4 kinase. PI-4 kinase is part of the canonical pathway for the synthesis of PIP2 by phosphorylating PI to PIP, which then serves as a substrate for the formation of PIP2 (Toker, 1998; Tolias and Carpenter, 2000). At the concentration used in our experiments (1 μM), PAO did not inhibit synaptic FM 4-64 loading and unloading; however, it prevented the increase in GFP fluorescence in presynaptic boutons upon stimulation ($n = 130$ from six experiments; Fig. 9). This effect was completely reversible by adding dithiothreitol (DTT; 2 mM). Wortmannin, which can also be used to inhibit PI-4 kinase, was found to interfere with FM 4-64 loading of synapses (even at the lower concentration used for inhibiting PI-3 kinase, 0.1 μM) and therefore could not be used for this experiment. The observed effect of PAO indicates that the increase in GFP fluorescence in stimulated presynaptic boutons depends on the synthesis of new PIP2.

NMDA receptor activation and subsequent NO production are needed for the increase in GFP fluorescence in stimulated presynaptic boutons

All the above experiments were performed in the presence of the α-amino-3-hydroxy-5-methyl-4-isoxazole propionic

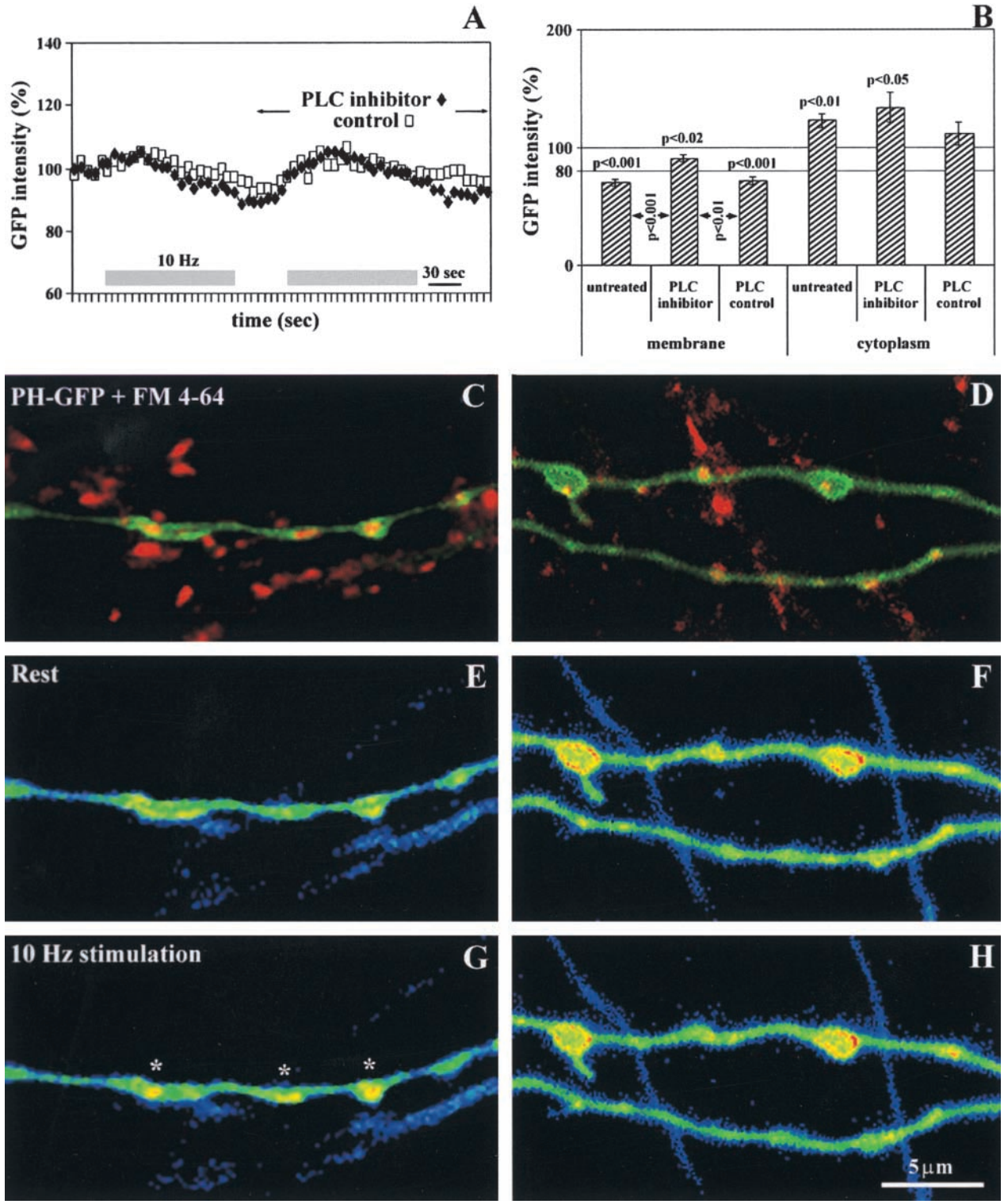

Figure 8. **Effect of PLC inhibition on the PH-GFP fluorescence of stimulated presynaptic boutons.** (A) Application of the PLC inhibitor U73122 (1 μM) does not affect the overall GFP fluorescence in presynaptic boutons. Neurons were stimulated first without and then with the PLC inhibitor U73122 or its positive control U73343. Values of GFP intensity were averaged across the synaptic population and normalized relative to the initial resting state. Only synapses showing an increase in GFP intensity in the first round of stimulation were chosen for the analysis ($n = 62$ for the PLC inhibitor, $n = 33$ for the control). (B) Application of the PLC inhibitor has an effect on the GFP fluorescence of the plasma membrane of presynaptic boutons. The values of GFP intensity for each condition are presented as percentage of the respective values at rest. The *P* values for the statistical significance of the difference between stimulation and rest are presented above each bar, and the difference between the various conditions during stimulation are shown between the respective bars. The application of the PLC inhibitor significantly decreased the drop in the plasma membrane GFP intensity upon stimulation, but did not affect the increase in the cytoplasmic GFP intensity. Please note that the membrane GFP intensity with the PLC inhibitor is higher than the baseline GFP intensity (corrected for the effect of pH). Error bars show standard errors. (C and D) Axons of hippocampal neurons (8 div), transfected with PH-GFP (green), and loaded with

acid/kainate receptor antagonist 6-cyano-7-nitroquinoxaline-2,3-dione (10 μM) to block spontaneous recurrent excitatory activity. To test for possible receptor dependence of the observed effects, we electrically stimulated transfected neurons in the presence of antagonists for the N-methyl-D-aspartate (NMDA) receptors (D[-]-2-Amino-5-phosphonopentanoic acid, 50 μm), group I/group II metabotropic glutamate receptors ([S]-α-methyl-4-carboxyphenylglycine, 1 mM), $GABA_A$ receptors (Bicuculline methobromide, 3 μM), and $GABA_B$ receptors (2-Hydroxysaclofen, 200 μM). Consistently, application of AP5 (50 μM) abolished the increase of GFP fluorescence in stimulated presynaptic boutons (n = 120 from six experiments), whereas the remaining antagonists did not have a detectable effect (Fig. 10 A). Since these results implicated NMDA receptors in mediating the effect of electrical stimulation on the production of PIP2, it was important to observe the distribution of NMDA receptors in our cultures. For this purpose, we performed a double immunolabeling of nontransfected hippocampal neurons with anti-NMDAR1 and antisynapsin antibodies (Fig.10, D and E). At the ages used for the stimulation experiments, NMDAR1 puncta were observed along dendrites, both at synaptic and extrasynaptic sites, and there was also a diffuse NMDAR1 labeling of cell bodies and larger dendrites. No consistent pattern of overlap was seen between the NMDAR1 and synapsin labeling, indicating an absence of NMDA receptors in presynaptic boutons, consistent with previous findings (Rao et al., 1998). Furthermore, retrospective staining of transfected neurons for NR1 revealed a strong correlation between the increase in GFP intensity of the presynaptic bouton upon electrical stimulation and the presence of NMDA receptors on the postsynaptic side (Fig. 10 F). Thus, 83% (57 out of 69) of presynaptic boutons that showed an increase in GFP intensity had adjacent NMDAR1-labeled punctae. These results are consistent with a role of NMDA receptor activation as a trigger for PIP2 synthesis in presynaptic boutons, and they also suggest that the process involves a retrograde messenger, for example nitric oxide (NO).

The production of NO by the enzyme neuronal NO synthase (NOS) is functionally coupled to Ca^{2+} influx through the NMDA receptors (Garthwaite and Boulton, 1995). To test for the involvement of NO, we stimulated transfected neurons in the presence of the NO scavenger 2-(4-carboxyphenyl)-4,4,5,5-tetramethylimidazoline-1-oxyl-3-oxide, potassium salt (carboxy-PTIO), which is cell membrane impermeable (Ko and Kelly, 1999) and does not affect NOS activity (Az-ma et al., 1994). Application of carboxy-PTIO (30 μM) during stimulation abolished the increase in GFP fluorescence in transfected presynaptic boutons, and this effect was reversible upon washing out (n = 65 from five experiments; Fig. 10 B). The selective neuronal NO synthase inhibitor 1-(2-trifluoromethylphenyl) imidazole (TRIM; 100 μM) had a similar effect, which was completely reversed upon application of L-arginine (1 mM; n = 36 from two experiments). Neither carboxy-PTIO nor TRIM at the concentrations used affected the unloading of the FM 4-64–labeled synapses.

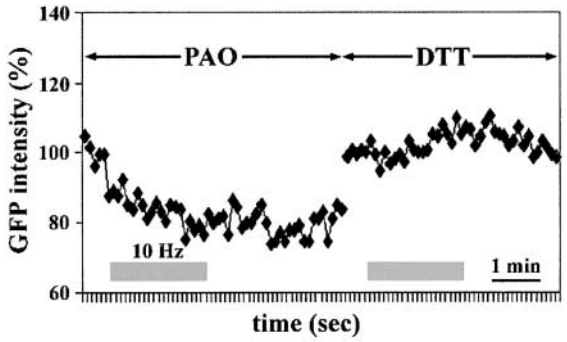

Figure 9. **The increase in PH-GFP fluorescence of stimulated presynaptic boutons depends on the synthesis of new PIP2.** Effect of PAO (1 μM) on the GFP fluorescence of stimulated synapses and its reversal by DTT (2 mM; n = 7). Values of GFP intensity were averaged across the synaptic population and normalized relative to the initial resting state. A representative individual experiment is shown.

The involvement of NO in the observed phenomenon was further confirmed by application of an NO donor to the neuronal cultures. The addition of diethylamine NO, sodium salt (DEANO; 100 μM) to the medium of PH-GFP–transfected neurons caused a large increase in the fluorescence intensity of presynaptic boutons (n = 100 from five experiments; Fig. 10 C). This increase was larger and lasted longer than the one caused by electrical stimulation. However, the effect was reversible after washing out the NO donor, and the viability of neurons was not impaired by this treatment, as assessed by an FM 4-64 loading–unloading protocol at the end of the experiment (result not shown).

These data strongly suggest that the upregulation of PIP2 concentration in stimulated boutons involves NO as a retrograde signal, which is produced upon activation of NMDA receptors.

Discussion

This study is, to our knowledge, the first observation in functional presynaptic terminals of the spatial distribution and dynamics of PIP2 as visualized with the PH-GFP probe. The following main findings are reported: (a) PIP2 is localized predominantly on the plasma membrane of resting neurons. (b) Synaptic activity causes a decrease of PIP2 concentration on the plasma membrane of synaptic boutons, most likely due to hydrolysis by PLC. (c) Synaptic activity also causes a pronounced increase in the PIP2 concentration inside the majority of boutons, where PIP2 is probably localized on freshly endocytosed membranes. (d) The increase of presynaptic PIP2 concentration by synaptic activity involves the activation of NMDA receptors and the retrograde action of NO.

FM 4-64 (red). (E–H) Pseudocolor images of these axons in the GFP channel during rest and electrical stimulation in the presence of the PLC inhibitor. Three out of the four presynaptic boutons in G showed an increase in GFP fluorescence upon stimulation (asterisks). The presynaptic boutons in H were chosen because they do not show the increase in cytoplasmic GFP intensity, which makes it easier to observe the changes specific to the plasma membrane.

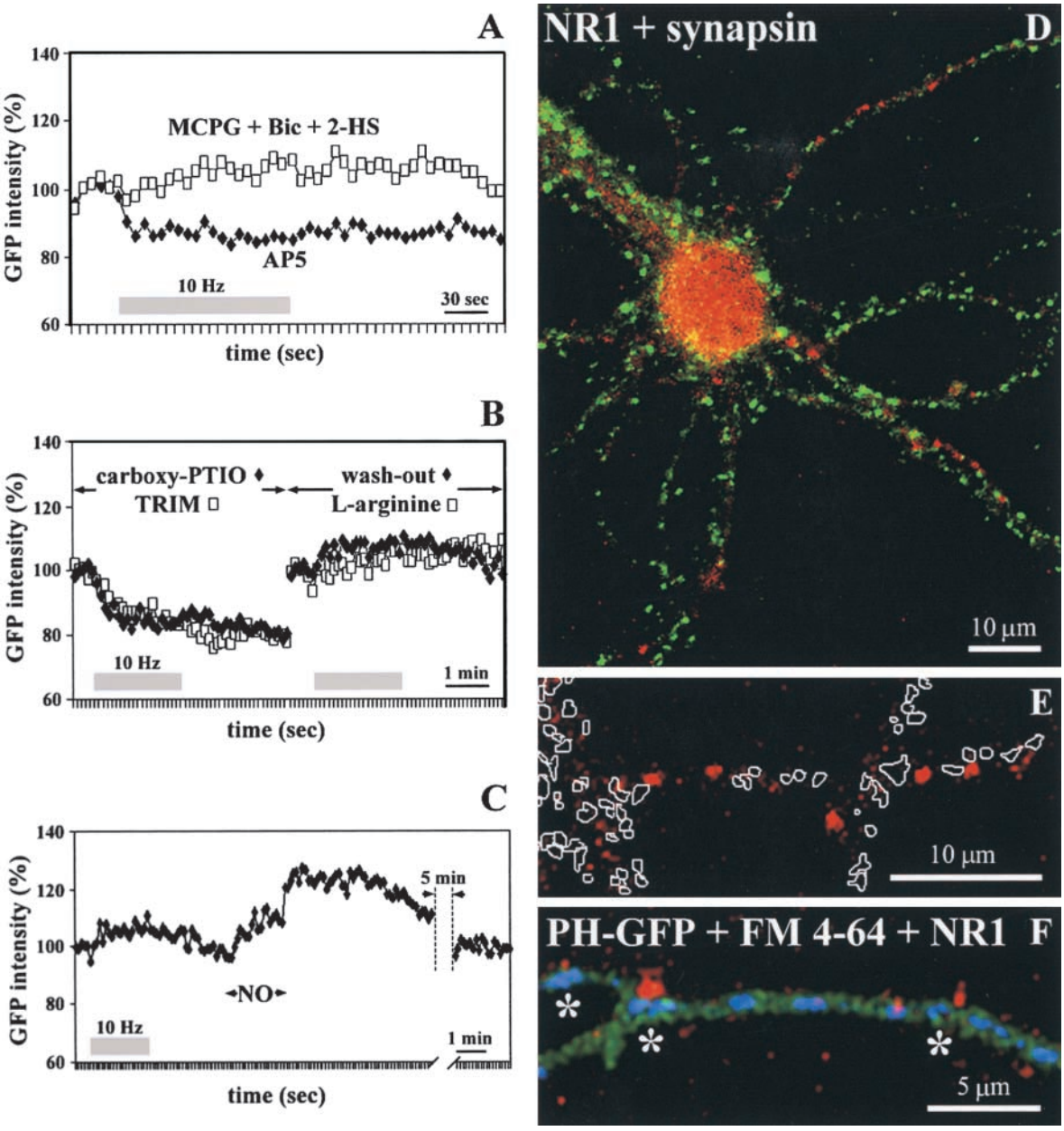

Figure 10. **NO is necessary for the increase in PH-GFP fluorescence in stimulated presynaptic boutons.** (A) Methyl-4-carboxyphenylglycine (1 mM), bicuculline (3 μM),and 2-hydroxysaclofen (200 μM) did not interfere with the increase in GFP fluorescence of stimulated synapses ($n = 13$), while AP5 (50 μM) abolished this response ($n = 21$). (B) Carboxy-PTIO (30 μM) and TRIM (100 μM) abolished the increase in GFP fluorescence of stimulated synapses, and this effect was reversible upon washing out or addition of L-arginine (1 mM), respectively ($n = 5$ for carboxy-PTIO and $n = 17$ for TRIM). (C) Addition of DEANO (100 μM) caused a large increase of the GFP fluorescence of synapses ($n = 18$). (A–C) Values of GFP intensity were averaged across the synaptic population and normalized relative to the initial resting state. Representative individual experiments are shown for each case. (D) Hippocampal neuron immunostained for synapsin (green) and NR1 (red). (E) A higher magnification view of neuronal processes in which synapsin punctae are outlined in white to show the lack of detectable overlap between synapsin and NR1 immunolabeling. (F) Axon of a hippocampal neuron transfected with PH-GFP (green) and loaded with FM 4-64 (blue). After the live experiment, the neurons were fixed and immunostained for NR1 (red). Asterisks mark the synapses, which showed an increase in GFP fluorescence during electrical stimulation.

Do the localization and intensity changes of PH-GFP reflect the spatial and temporal dynamics of PIP2?

The PH domain of PLC δ1 has been shown to bind specifically and with high affinity to PIP2 and has been used successfully in previous studies to visualize PIP2 in nonneuronal cells (Stauffer et al., 1998; Varnai and Balla, 1998; Botelho et al., 2000; Holz et al., 2000; Raucher et al., 2000). The typical plasma membrane distribution of PH-GFP described in these studies was also observed in resting hippocampal neurons. Furthermore, the localization of PIP2 as identified with a monoclonal antibody in fixed nontransfected neurons was identical to the distribution of PH-GFP in transfected neurons, providing strong support for the use of this construct as a probe for PIP2. In addition, we ob-

served that actin polymerization was partially impaired in the neurons transfected with PH-GFP, which is consistent with previous studies showing that depleting PIP2 leads to actin disassembly (Flanagan and Janmey, 2000).

The changes in the pattern and intensity of PH-GFP fluorescence upon stimulation also appear to be due to the binding of the probe to PIP2. Thus, inhibiting PI-4 kinase, which is necessary for the production of PIP2, abolishes the increase of PH-GFP fluorescence upon stimulation. And even though the PH domain of PLC δ1 also has a very high affinity to IP3 (Cifuentes et al., 1994; Yagisawa et al., 1994; Lemmon et al., 1995), we do not believe that a competitive binding of PH-GFP to IP3 can account for the observed events, since inhibiting PLC and thus blocking the production of IP3 did not affect the increase in cytoplasmic GFP intensity in firing presynaptic boutons. Rather, the increase in the PH-GFP fluorescence within the cytoplasm of presynaptic boutons is most probably due to the diffusion of PH-GFP from adjacent areas driven by the increased concentration of PIP2. The relatively high mobility of PH-GFP, as revealed by the photobleaching experiments, can easily account for such an increase. Therefore, the dynamics of PH-GFP in our system are most likely a reflection of dynamics of PIP2.

Another issue is whether PH-GFP can detect all neuronal pools of PIP2. For example, PIP2 could be binding to other proteins, rendering it unavailable to PH-GFP. Thus, the lack of detectable PH-GFP labeling of synaptic vesicles in quiescent neurons cannot be necessarily interpreted as a lack of PIP2. However, this observation indicates the lack of an easily accessible pool of PIP2 on synaptic vesicles, i.e., if PIP2 is present there, it is masked by binding to other proteins and is not readily available for other interactions. Taking all these considerations into account, we believe that in the present system PH-GFP is an excellent probe for visualizing the dynamics of the accessible pool of PIP2, i.e., the "active" PIP2 available, for example, as a substrate for PLC and other enzymes or as a recruiter of proteins involved in endocytosis. Keeping these methodological issues in mind, in the Discussion we will refer to the PH-GFP fluorescence as the PIP2 signal for the sake of clarity.

Dynamics of presynaptic PIP2

Confocal imaging of PIP2, as labeled with PH-GFP, revealed the specific localization and dynamics of this phospholipid in live hippocampal neurons. In resting neurons, the PIP2 signal was concentrated on the plasma membrane. However, electrical stimulation triggered a series of events affecting both the distribution and the intensity of the PIP2 signal in the presynaptic bouton. Immediately after the onset of stimulation, the PIP2 signal of the plasma membrane decreased significantly and this event depended on the activation of PLC. In vitro and in situ studies have shown that PLC can be activated by Ca^{2+} (for review see Eberhard and Holz, 1988) and that among all PLC isoforms, PLC-δ, which binds to the plasma membrane PIP2 through its PH domain, is the most sensitive to Ca^{2+} (for review see Rhee et al., 2000). Therefore, an increase in the Ca^{2+} concentration within the firing presynaptic bouton might activate PLC-δ and lead to the hydrolysis of the plasma membrane PIP2 to diacylglycerol and IP3, thus resulting in a decreased PIP2 concentration on the plasma membrane and also triggering a series of second messenger cascades.

Within seconds after the beginning of stimulation there was, in addition to a decrease in the plasma membrane PIP2 signal, a substantial increase of the signal in the cytoplasmic domain of boutons. This increase was correlated, albeit weakly, to the number of recycling vesicles and most probably was also influenced by the different molecular composition and history of synapses. Further investigation into the possible mechanisms of this event revealed that it depended on the activation of NMDA receptors and a retrograde action of NO. Indeed, we observed an excellent correlation between the presence of NMDA receptors at the postsynaptic side of the synaptic junction and the increase in PIP2 signal at the presynaptic site.

A more difficult question to answer at the present moment is how NO affects PIP2 concentration. Our experiments show that synthesis of new PIP2 is required; however, keeping in mind that there is a constant turnover of PIP2 at the active synapse (Stenmark, 2000), both increasing the rate of its production and slowing the rate of its hydrolysis will result in an overall increase of its concentration. A major target of NO in the brain is guanylyl cyclase, responsible for the production of cGMP, which, on its turn, can participate in channel gating and in the regulation of numerous enzymes, such as protein kinases, phosphodiesterases, and ADP ribosyl cyclase (for review see Garthwaite and Boulton, 1995). One documented link between NO and PIP2 is the negative modulation of PIP2 hydrolysis, possibly achieved by a cGMP-dependent protein kinase I acting at the level of PLC (Clementi et al., 1995). By blocking PIP2 hydrolysis, NO would cause an increase in PIP2 concentration as observed in this study. Taking into account the relatively long chain of events needed for this effect to take place, this would allow sufficient time for the above-described PLC hydrolysis of plasma membrane PIP2 first to occur. Alternatively, presynaptic PIP2 concentration might increase if NO were to stimulate the production of new PIP2. The main pathway of PIP2 synthesis in cells appears to be through PI(4)P. Two families of enzymes are involved in this process: PI-4 kinases, which phosphorylate phosphatidylinositol on the D-4 position of the inositol ring to produce PI(4)P, and phosphatidylinositol 4–phosphate-5 kinases, which phosphorylate PI(4)P to PI(4,5P)2 (Tolias and Carpenter, 2000). In the present study, blocking of PI-4 kinases by PAO prevents the increase in PIP2 in response to synaptic activity, suggesting that this is the main pathway for PIP2 synthesis in presynaptic boutons. It is unknown whether NO stimulates either enzyme in the pathway.

The increase in the presynaptic PIP2 signal in response to stimulation is consistent with a role for PIP2 in the endocytosis of synaptic vesicles

A major finding of the present study is that prolonged synaptic activity caused a significant increase in the cytoplasmic PIP2 signal in the majority of presynaptic boutons. This increase was observed only in active synapses, as identified by loading with FM 4-64. It occurred on average 20 s after the beginning of electrical stimulation and continued well after

the end of stimulation (~2 min after a 2 min stimulation of 10 Hz). Presynaptic boutons with a larger number of recycling vesicles were much more likely to display such an increase in GFP fluorescence. The localization and time course of the increase in PIP2 signal correlates well with the suggested role for PIP2 in synaptic vesicle endocytosis. PIP2 has been implicated at almost all steps of synaptic vesicle endocytosis, such as the formation of the endocytic clathrin coat via the PIP2 interaction with AP180, epsin, and AP2 (Gaidarov and Keen, 1999; Ford et al., 2001; Itoh et al., 2001); the fission of the neck of the coated pit via the PIP2 interaction with dynamin (Lin and Gilman, 1996; Zheng et al., 1996); the uncoating of the endocytosed vesicle requiring the hydrolysis of PIP2 by synaptojanin (Cremona et al., 1999); and in the transport of the endocytic vesicle because of the PIP2 dependence of actin assembly (Rozelle et al., 2000). Therefore, it is possible that the increased demand on the endocytic machinery caused by prolonged synaptic activity and a large number of recycling vesicles would require higher concentrations of PIP2.

The increase in PIP2 concentration consistently occurred within presynaptic boutons, and not on the plasma membrane. This is likely to be due to the accumulation of newly endocytosed clathrin-coated vesicles containing PIP2 in their membrane. Because PIP2 must be metabolized by the lipid phosphatase synaptojanin in order for the uncoating of endocytic vesicles to occur (Cremona et al., 1999), mature synaptic vesicles may be devoid of PIP2. Indeed, the PIP2 signal did not colocalize with mature, FM 4-64–labeled synaptic vesicles. Thus, our experiments may reflect part of a PIP2 cycle in which synthesis occurs on the plasma membrane after exocytosis and increased levels of PIP2 facilitate endocytosis. The PIP2 synthesis on the plasma membrane, however, is masked by the simultaneously occurring PLC activation and the pinching off of clathrin-coated vesicles carrying away PIP2. Indeed, inhibiting PLC reveals a significant increase in the PIP2 signal of the plasma membrane in stimulated presynaptic boutons (13% increase when adjusted for the effect of pH on GFP). PIP2-containing clathrin-coated vesicles transiently accumulate in the cytoplasm of presynaptic boutons, thus accounting for the increase in PIP2 signal seen within stimulated boutons. Degradation of PIP2 by synaptojanin then occurs, allowing the uncoating of vesicles and their repriming for exocytosis, and can be observed as a decrease in the PIP2 signal. In addition, the increase in the PIP2 signal within stimulated boutons may also be due to the accumulation of endocytic intermediates, called cisternae or vacuoles (Koenig and Ikeda, 1996; Takei et al., 1996), thought to be derived from plasma membrane taken up in bulk. As derivatives from the plasma membrane, endocytic cisternae most probably contain PIP2, and it may even be actively synthesized there in order to facilitate the formation of clathrin-coated vesicles. The precise localization of PH-GFP within stimulated boutons will require further confirmation by immunocytochemistry on the electron microscopic level.

Because of the involvement of PIP2 in synaptic vesicle recycling, it might seem surprising that we did not observe defects in synaptic function upon expression of PH-GFP in hippocampal neurons. In contrast, expression of PH-GFP in neuroendocrine cells inhibited exocytosis (Holz et al., 2000). One possible explanation is that the cells we selected for analysis had relatively low levels of expression (see Materials and methods) and the sequestration of a small portion of PIP2 molecules therefore had little or no functional consequence. Alternatively, this may be a reflection of a real functional difference between neuroendocrine cells and hippocampal neurons.

The regulation of presynaptic PIP2 concentration by NMDA receptor activation and a retrograde action of NO may be involved in activity-dependent synaptic plasticity

In the present study we have described a new pathway for retrograde signaling at the synapse, i.e., the activation of NMDA receptors by high levels of synaptic activity leads to the production of NO at the postsynaptic side, which then diffuses to the presynaptic side and causes an increase in PIP2 concentration. What may be the functional significance of an NO-mediated regulation of presynaptic PIP2 levels? The exact roles of NO in the central nervous system are still a matter of dispute, but it has been implicated in synaptic plasticity, including LTP, in neuronal development, and in neurotoxicity (for review see Schuman and Madison, 1994; Jaffrey and Snyder, 1995; Garthwaite and Boulton, 1995). Among the well-described effects of NO in the central nervous system is its capability to elicit or increase neurotransmitter release in a variety of systems. Our results suggest that, in parallel to regulating neurotransmitter release, NO may also regulate the presynaptic PIP2 concentration, possibly to provide adequate amounts of this phospholipid needed for synaptic vesicle recycling. In addition, increasing the concentration of PIP2 will stimulate actin assembly and thus may be involved in such activity-dependent morphological rearrangements of the presynaptic bouton as formation of perforated synapses and even synapse multiplication (for review see Geinisman, 2000).

Materials and methods

Cell culture and transfection

Primary embryonic hippocampal cultures were prepared as in Goslin et al. (1998). Cells were transfected using a modified calcium phosphate transfection protocol (Xia et al., 1996). The plasmids encoding the PH domain of PLCδ_1 fused to GFP (PH-GFP) or the mutant PH(S34T, R40L)-GFP were a gift of Dr. Tamas Balla (Endocrinology and Reproduction Research Branch, NICHD, NIH, Bethesda, MD) (Varnai and Balla, 1998). Typically, 5–10% transfection rates were obtained. For these experiments, cells within the lower to middle range of GFP expression were selected to avoid possible artifacts associated with high levels of expression.

Immunostaining

Due to the labile nature of this phospholipid, for PIP2 immunostaining the cells were fixed using rapid microwave irradiation (PELCO 3451 laboratory microwave system; Ted Pella, Inc.; two cycles of 8 s on, 20 s off, 8 s on) in 1% glutaraldehyde and 4% paraformaldehyde in PBS on ice. After rinsing in PBS buffer, the cells were quenched in 20 mM glycine for 5 min, rinsed again and permeabilized, and then blocked in a solution of 5% normal goat serum (NGS) and 0.1% saponin in PBS for 1 h. The cells were then incubated in the primary antibody (1:500 in PBS with 1% NGS) for 2 h at room temperature, rinsed well in PBS, and incubated in fluorescent-labeled secondary antibody for 1 h at room temperature.

For all other immunostaining, the cells were fixed in methanol for 15 min at −20°C, incubated in blocking medium (5% NGS and 5% bovine serum albumin in PBS) for 1 h at 37°C followed by incubation in primary antibody diluted in 1% NGS in PBS for 2 h at room temperature, and incubation in the appropriate fluorescent-labeled secondary antibody for 1 h at room temperature. After each step the cells were washed in PBS. The fol-

lowing antibodies were used: monoclonal mouse anti-PIP2 (Assay Designs; 1:500), monoclonal mouse antisynapsin I (Chemicon; 1:400), polyclonal rabbit antisynapsin I (Chemicon; 1:1,000), monoclonal mouse antiglutamate receptor (NMDAR1; PharMingen International; 1:200), and Cy5-conjugated goat anti–mouse or anti–rabbit IgG (Jackson ImmunoResearch Laboratories; 1:800).

To visualize actin, the cells were fixed in 4% paraformaldehyde in PBS for 20 min at 4°C, permeabilized with 0.3% Triton X-100 in PBS for 5 min at room temperature, blocked with 5% NGS and 5% bovine serum albumin in PBS for 1 h at 37°C, and then incubated in Bodipy 650/665 phalloidin (Molecular Probes) for 30 min at room temperature. After each step the cells were washed in PBS.

Microscopy, photobleaching, and FM 4-64 loading

Coverslips were mounted in a custom-built imaging chamber with 500 μl of prewarmed (37°C) Tyrode's saline solution (119 mM NaCl, 2.5 mM KCl, 2 mM $CaCl_2$, 2 mM $MgCl_2$, 25 mM HEPES, buffered to pH 7.4) with 30 mM glucose, 1% chicken albumin (Sigma-Aldrich) and 10 μM 6-cyano-7-nitroquinoxaline-2,3-dione (CNQX; Tocris). During imaging, cells were kept at 37°C. Imaging was done with a scanning laser confocal microscope designed by S.J. Smith using a ZEISS 40×/1.3 NA Fluar objective or a 63×/1.4 NA PlanApochromat objective. Microscope control software was written by Dr. Noam E. Ziv (Technion, Haifa, Israel). Unless otherwise stated, an electronic zoom of 2× with pixel size 0.286 μm was used during the experiments. Images were collected every 6 s. To protect the specimen from photodamage, and taking into account the flat nature of the preparation and the generally small size of presynaptic boutons, only one z-section was collected at each time point. To assure further that fluorescence from entire synapses could be captured accurately in single optical sections, a large detection pinhole (4 μm referred to the specimen plane) was used in all experiments, except for the high resolution imaging of large presynaptic terminals.

For photobleaching experiments, 12-μm stretches of transfected axons were bleached using a very high zoom (30×, pixel size 0.019 μm) and power (~400 mW, 488-nm wavelength). The recovery was monitored at a lower zoom (15×, pixel size 0.038 μm) and power (20 mW, 488-nm wavelength). Average fluorescence intensity data from the bleached regions were collected from each frame before the bleaching and during the recovery.

To identify functional synapses, the fluorescent styryl dye FM 4-64 (Molecular Probes) was used. The membrane probe FM 4-64 becomes internalized within recycled synaptic vesicles and thus stains active synapses, which undergo exo- and endocytosis (Betz et al., 1992; Murthy, 1999). The dye was superfused into the chamber at a concentration of 5 μM and the neurons were electrically stimulated by passing current pulses between electrodes placed at opposite ends of the perfusion chamber (see Ryan and Smith, 1995). Unless otherwise noted, 10 Hz stimulation for 30 s was applied. After an additional 30 s, the dye was washed away. Regions of transfected axons making synaptic contacts were then selected and time-lapse imaged at rest and during electrical stimulation (10 Hz for 2 min). FM loading was determined by subtracting from the initial FM values the residual FM values obtained after the second electrical stimulation, which "unloaded" the presynaptic boutons.

Pharmacology

The effect of the following reagents was tested: PLC inhibitor U73122 (Sigma-Aldrich; 1 μM) and its analogue U73343 (Sigma-Aldrich; 1 μM); PAO (Sigma-Aldrich; 1 μM); DTT (Sigma-Aldrich; 2 mM); D(-)-2-Amino-5-phosphonopentanoic acid (Tocris; 50 μm); (S)-α-Methyl-4-carboxyphenylglycine (Tocris; 1 mM); bicuculline methobromide (Tocris, 3 μM); 2-hydroxysaclofen (Tocris; 200 μM); carboxy-PTIO (Molecular Probes; 30 μM); TRIM (Molecular Probes, Eugene, Oregon; 100 μM); and DEANO (Molecular Probes; 100 μM).

Image analysis

Images were analyzed with custom software (N.E. Ziv, Technion). For the analysis of the dynamics of GFP fluorescence in presynaptic boutons, average fluorescence intensities from 4 × 4 or 6 × 6 pixel squares centered on presynaptic boutons were collected from each frame. The data for each bouton were normalized relative to the first five frames taken at rest. For the analysis of large presynaptic varicosities, average fluorescence intensities from seven randomly chosen pixels on the plasma membrane or in the cytoplasm were collected and then normalized relative to the resting state.

We thank Dr. Tamas Balla for his kind gift of the GFP constructs, Dr. James Jontes for critical reading of the manuscript, and Mr. Yemane Gedde for excellent technical assistance.

This work was supported by grants from the National Institute of Mental Health (NS28587 and Silvio Conte Center for Neuroscience Research, MH48108) and the Mathers Foundation to S.J. Smith, and National Institutes of Health grants R01-DK50127 and RO1-DK27959 to R.W. Holz. The participation of R.W. Holz in this study occurred during a sabbatical in the laboratory of S.J. Smith.

Submitted: 16 February 2001
Revised: 14 May 2001
Accepted: 13 June 2001

References

Az-ma, T., K. Fujii, and O. Yuge. 1994. Reaction between imidazolineoxil N-oxide (carboxy-PTIO) and nitric oxide released from cultured endothelial cells: quantitative measurement of nitric oxide by ESR spectrometry. *Life Sci.* 54: PL185–PL190.

Betz, W.J., F. Mao, and G.S. Bewick. 1992. Activity-dependent fluorescent staining and destaining of living motor nerve terminals. *J. Neurosci.* 12:363–375.

Botelho, R.J., M. Teruel, R. Dierckman, R. Anderson, A. Wells, J.D. York, T. Meyer, and S. Grinstein. 2000. Localized biphasic changes in phosphatidylinositol-4,5-bisphosphate at sites of phagocytosis. *J. Cell Biol.* 151:1353–1367.

Chesler, M., and K. Kaila. 1992. Modulation of pH by neuronal activity. *Trends Neurosci.* 15:396–402.

Chung, S.H., W.J. Song, K. Kim, J.J. Bednarski, J. Chen, G.D. Prestwich, and R.W. Holz. 1998. The C2 domains of Rabphilin3A specifically bind phosphatidylinositol 4,5-bisphosphate containing vesicles in a Ca^{2+}-dependent manner. In vitro characteristics and possible significance. *J. Biol. Chem.* 273: 10240–10248.

Cifuentes, M.E., T. Delaney, and M.J. Rebecchi. 1994. D-myo-inositol 1,4,5-trisphosphate inhibits binding of phospholipase C-δ1 to bilayer membranes. *J. Biol. Chem.* 269:1945–1948.

Clementi, E., C. Sciorati, M. Riccio, M. Miloso, J. Meldolesi, and G. Nisticò. 1995. Nitric oxide action on growth factor-elicited signals. Phosphoinositide hydrolysis and $[Ca^{2+}]$i responses are negatively modulated via a cGMP-dependent protein kinase I pathway. *J. Biol. Chem.* 270:22277–22282.

Corvera, S., A. D'Arrigo, and H. Stenmark. 1999. Phosphoinositides in membrane traffic. *Curr. Opin. Cell Biol.* 11:460–465.

Cremona, O., and P. De Camilli. 2001. Phosphoinositides in membrane traffic at the synapse. *J. Cell Sci.* 114:1041–1052.

Cremona, O., G.D. Paolo, M.R. Wenk, A. Luthi, W.T. Kim, K. Takei, L. Daniell, Y. Nemoto, S.B. Shears, R.A. Flavell, D.A. McCormick, and P.D. Camilli. 1999. Essential role of phosphoinositide metabolism in synaptic vesicle recycling. *Cell.* 99:179–188.

Eberhard, D.A., and R.W. Holz. 1988. Intracellular calcium can activate phospholipase C. *Trends Neurosci.* 11:517–520.

Eberhard, D.A., C.L. Cooper, M.G. Low, and R.W. Holz. 1990. Evidence that the inositol phospholipids are necessary for exocytosis. Loss of inositol phospholipids and inhibition of secretion in permeabilized cells caused by a bacterial phospholipase C and removal of ATP. *Biochem. J.* 268:15–25.

Eichberg, J., and R.M. Dawson. 1965. Polyphosphoinositides in myelin. *Biochem. J.* 96:644–650.

Flanagan, L., and P.A. Janmey. 2000. Regulation of cytoskeletal proteins by inositol lipids. *In* Biology of Phosphoinositides. Vol. 27. S. Cockcroft, editor. Oxford University Press, Oxford, England. 166–182.

Ford, M.G.J., B.M.F. Pearse, M.K. Higgins, Y. Vallis, D.J. Owen, A. Gibson, C.R. Hopkins, P.R. Evans, and H.T. McMahon. 2001. Simultaneous binding of PtdIns(4,5)P2 and clathrin by AP180 in the nucleation of clathrin lattices on membranes. *Science.* 291:1051–1055.

Gaidarov, I., and J.H. Keen. 1999. Phosphoinositide-AP-2 interactions required for targeting to plasma membrane clathrin-coated pits. *J. Cell Biol.* 146:755–764.

Garthwaite, J., and C.L. Boulton. 1995. Nitric oxide signaling in the central nervous system. *Annu. Rev. Physiol.* 57:683–706.

Geinisman, Y. 2000. Structural synaptic modifications associated with hippocampal LTP and behavioral learning. *Cereb. Cortex.* 10:952–962.

Goslin, K., H. Asmussen, and G. Banker. 1998. Rat hippocampal neurons in low-density culture. *In* Culturing Nerve Cells. G. Banker and K. Goslin, editors. The MIT Press, Cambridge, MA. 339–370.

Gross, S.D., D.P. Hoffman, P.L. Fisette, P. Baas, and R.A. Anderson. 1995. A phosphatidylinositol 4,5-bisphosphate-sensitive casein kinase I alpha associates with synaptic vesicles and phosphorylates a subset of vesicle proteins. *J.*

Cell Biol. 130:711–724.

Hay, J.C., P.L. Fisette, G.H. Jenkins, K. Fukami, T. Takenawa, R.A. Anderson, and T.F. Martin. 1995. ATP-dependent inositide phosphorylation required for Ca(2+)-activated secretion. *Nature.* 374:173–177.

Hokin, L., and M.R. Hokin. 1964. *Biochim. Biophys. Acta.* 84:563–575.

Holz, R.W., M.A. Bittner, S.C. Peppers, R.A. Senter, and D.A. Eberhard. 1989. MgATP-independent and MgATP-dependent exocytosis: evidence that MgATP primes adrenal chromaffin cells to undergo exocytosis. *J. Biol. Chem.* 264:5412–5419.

Holz, R.W., M.D. Hlubek, S.D. Sorensen, S.K. Fisher, T. Balla, S. Ozaki, G.D. Prestwich, E.L. Stuenkel, and M.A. Bittner. 2000. A pleckstrin homology domain specific for phosphatidylinositol 4,5-bisphosphate (PtdIns-4,5-P2) and fused to green fluorescent protein identifies plasma membrane PtdIns-4,5-P2 as being important in exocytosis. *J. Biol. Chem.* 275:17878–17885.

Itoh, T., S. Koshiba, T. Kigawa, A. Kikuchi, S. Yokoyama, and T. Takenawa. 2001. Role of the ENTH domain in phosphatidylinositol-4,5-biphosphate binding and endocytosis. *Science.* 291:1047–1051.

Jaffrey, S.R., and S.H. Snyder. 1995. Nitric oxide: a neural messenger. *Annu. Rev. Cell Dev. Biol.* 11:417–440.

Jost, M., F. Simpson, J.M. Kavran, M.A. Lemmon, and S.L. Schmid. 1998. Phosphatidylinositol-4,5-bisphosphate is required for endocytic coated vesicle formation. *Curr. Biol.* 8:1399–1402.

Ko, G.Y., and P.T. Kelly. 1999. Nitric oxide acts as a postsynaptic signaling molecule in calcium/calmodulin-induced synaptic potentiation in hippocampal CA1 pyramidal neurons. *J. Neurosci.* 19:6784–6794.

Koenig, J.H., and K. Ikeda. 1996. Synaptic vesicles have two distinct recycling pathways. *J. Cell Biol.* 135:797–808.

Lemmon, M.A., K.M. Ferguson, R. O'Brien, P.B. Sigler, and J. Schlessinger. 1995. Specific and high-affinity binding of inositol phosphates to an isolated pleckstrin homology domain. *Proc. Natl Acad. Sci. USA.* 92:10472–10476.

Lin, H.C., and A.G. Gilman. 1996. Regulation of dynamin I GTPase activity by G protein βγ subunits and phosphatidylinositol 4,5-biphosphate. *J. Biol. Chem.* 271:27979–27982.

Loyet, K.M., J.A. Kowalchyk, A. Chaudhary, J. Chen, G.D. Prestwich, and T.F.J. Martin. 1998. Specific binding of phosphatidylinositol 4,5-bisphosphate to calcium-dependent activator protein for secretion (CAPS), a potential phosphoinositide effector protein for regulated exocytosis. *J. Biol. Chem.* 273: 8337–8343.

Martin, T.F.J. 1998. Phosphoinositide lipids as signaling molecules: common themes for signal transduction, cytoskeletal regulation, and membrane trafficking. *Annu. Rev. Cell Dev. Biol.* 14:231–264.

McPherson, P.S., E.P. Garcia, V.I. Slepnev, C. David, X. Zhang, D. Grabs, W.S. Sossin, R. Bauerfeind, Y. Nemoto, and P.D. Camilli. 1996. A presynaptic inositol-5-phosphatase. *Nature.* 379:353–357.

Murthy, V.N. 1999. Optical detection of synaptic vesicle exocytosis and endocytosis. *Curr. Opin. Neurobiol.* 9:314–320.

Okamoto, M., and T.C. Sudhof. 1997. Mints, Munc18-interacting proteins in synaptic vesicle exocytosis. *J. Biol. Chem.* 272:31459–31464.

Paterson, H.F., J.W. Savopoulos, O. Perisic, R. Cheung, M.V. Ellis, R.L. Williams, and M. Katan. 1995. Phospholipase C δ1 requires a pleckstrin homology domain for interaction with the plasma membrane. *Biochem. J.* 312: 661–666.

Patterson, G.H., S.M. Knobel, W.D. Sharif, S.R. Kain, and D.W. Piston. 1997. Use of the green fluorescent protein and its mutants in quantitative fluorescence microscopy. *Biophys. J.* 73:2782–2790.

Raucher, D., T. Stauffer, W. Chen, K. Shen, S. Guo, J.D. York, M.P. Sheetz, and T. Meyer. 2000. Phosphatidylinositol 4,5-biphosphate functions as a second messenger that regulates cytoskeleton-plasma membrane adhesion. *Cell.* 100:221–228.

Rao, A., E. Kim, M. Sheng, and A.-M. Craig. 1998. Heterogeneity in the molecular composition of excitatory postsynaptic sites during development of hippocampal neurons in culture. *J. Neurosci.* 18:1217–1229.

Rhee, S.G., B. Poulin, S.B. Lee, and F. Sekiya. 2000. Regulation of phosphoinositide-specific phospholipase C isoenzymes. *In* Biology of Phosphoinositides. Vol. 27. S. Cockcroft, editor. Oxford University Press, Oxford, England. 1–31.

Rozelle, A.L., L.M. Machesky, M. Yamamoto, M.H. Driessens, R.H. Insall, M.G. Roth, K. Luby-Phelps, G. Marriott, A. Hall, and H.L. Yin. 2000. Phosphatidylinositol 4,5-biphosphate induces actin-based movement of raft-enriched vesicles through WASP-Arp2/3. *Curr. Biol.* 10:311–320.

Ryan, T.A., and S.J. Smith. 1995. Vesicle pool mobilization during action potential firing at hippocampal synapses. *Neuron.* 14:983–989.

Schiavo, G., Q.M. Gu, G.D. Prestwich, T.H. Sollner, and J.E. Rothman. 1996. Calcium-dependent switching of the specificity of phosphoinositide binding to synaptotagmin. *Proc. Natl Acad. Sci. USA.* 93:13327–13332.

Schmidt, A., M. Wolde, C. Thiele, W. Fest, H. Kratzin, A.V. Podtelejnikov, W. Witke, W.B. Huttner, and H.D. Soling. 1999. Endophilin I mediates synaptic vesicle formation by transfer of arachidonate to lysophosphatidic acid. *Nature.* 401:133–141.

Schuman, E.M., and D.V. Madison. 1994. Nitric oxide and synaptic function. *Annu. Rev. Neurosci.* 17:153–183.

Stauffer, T.P., S. Ahn, and T. Meyer. 1998. Receptor-induced transient reduction in plasma membrane PtdIns(4,5)P2 concentration monitored in living cells. *Curr. Biol.* 8:343–346.

Stenmark, H. 2000. Cycling lipids. *Curr. Biol.* 10:R57–R59.

Takei, K., O. Mundigl, L. Daniell, and P. De Camilli. 1996. The synaptic vesicle cycle: a single vesicle budding step involving clathrin and dynamin. *J. Cell Biol.* 133:1237–1250.

Toker, A. 1998. The synthesis and cellular roles of phosphatidylinositol 4,5-biphosphate. *Curr. Opin. Cell Biol.* 10:254–261.

Tolias, K.F., and C.L. Carpenter. 2000. Enzymes involved in the synthesis of PtdIns(4,5)P2 and their regulation: PtdIns kinases and PtdInsP kinases. *In* Biology of Phosphoinositides. Vol. 27. S. Cockcroft, editor. Oxford University Press, Oxford, England. 109–130.

Varnai, P., and T. Balla. 1998. Visualization of phosphoinositides that bind pleckstrin homology domains: calcium- and agonist-induced dynamic changes and relationship to myo-[^{3}H]inositol-labeled phosphoinositide pools. *J. Cell Biol.* 143:501–510.

Waring, M., J. Drappatz, O. Weichel, P. Seimetz, E. Sarri, I. Bockmann, U. Kempter, A. Valeva, and J. Klein. 1999. Modulation of neuronal phospholipase D activity under depolarizing conditions. *FEBS Lett.* 464:21–24.

Wiedemann, C., T. Schäfer, M.M. Burger, and T.S. Sihra. 1998. An essential role for a small synaptic vesicle-associated phosphatidylinositol 4-kinase in neurotransmitter release. *J. Neurosci.* 18:5594–5602.

Xia, Z., H. Dudek, C.K. Miranti, and M.E. Greenberg. 1996. Calcium influx via the NMDA receptor induces immediate early gene transcription by a MAP kinase/ERK-dependent mechanism. *J. Neurosci.* 16:5425–5436.

Xiong, Z.-Q., P. Saggau, and J.L. Stringer. 2000. Activity-dependent intracellular acidification correlates with the duration of seizure activity. *J. Neurosci.* 20: 1290–1296.

Yagisawa, H., M. Hirata, T. Kanematsu, Y. Watanabe, S. Ozaki, K. Sakuma, H. Tanaka, N. Yabuta, H. Kamata, and H. Hirata. 1994. Expression and characterization of an inositol 1,4,5-trisphosphate binding domain of phosphatidylinositol-specific phospholipase C-δ1. *J. Biol. Chem.* 269:20179–20188.

Zhan, R.Z., N. Fujiwara, E. Tanaka, and K. Shimoji. 1998. Intracellular acidification induced by membrane depolarization in rat hippocampal slices: roles of intracellular Ca^{2+} and glycolysis. *Brain Res.* 780:86–94.

Zheng, J., S.M. Cahill, M.A. Lemmon, D. Fushman, J. Schlessinger, and D. Cowburn. 1996. Identification of the binding site for acidic phospholipids on the PH domain of dynamin: implications for stimulation of GTPase activity. *J. Mol. Biol.* 255:14–21.